SCIENCE CHINA
Information Sciences

• RESEARCH PAPER •

August 2018, Vol. 61 082301:1–082301:13
https://doi.org/10.1007/s11432-017-9259-0

BER analysis of STBC hybrid carrier system based on WFRFT with frequency domain equalization

Zhenduo WANG[1,2], Lin MEI[1*], Xuejun SHA[1] & Naitong ZHANG[1]

[1]*Communication Research Center, Harbin Institute of Technology, Harbin* 150001*, China;*
[2]*Science and Technology on Information Transmission and Dissemination in Communication Networks Laboratory, Shijiazhuang* 050081*, China*

Received 23 May 2017/Revised 8 August 2017/Accepted 10 October 2017/Published online 18 May 2018

Abstract The inherent characteristic of hybrid carrier (HC) scheme based on the weighted-type fractional Fourier transform (WFRFT) is revealed. The proposed linear combination of single carrier (SC) and multi-carrier's (MC) characteristics is helpful to balance the conflicting requirements and achieve the comparative analysis of SC/MC. As an example, analytical SER/BER expressions of HC system with zero forcing (ZF) and minimum mean square error (MMSE) equalization are derived. In addition, the derived BER expressions are extended to multi-input systems. A unified framework of space time block code (STBC) HC scheme is proposed with two WFRFT modules at the transmitter or receiver, where STBC-SC and STBC-MC systems are the special cases of the novel structure.

Keywords single carrier, multi-carrier, weighted-type fractional Fourier transform, hybrid carrier, zero forcing, minimum mean square error, space time block code

Citation Wang Z D, Mei L, Sha X J, et al. BER analysis of STBC hybrid carrier system based on WFRFT with frequency domain equalization. Sci China Inf Sci, 2018, 61(8): 082301, https://doi.org/10.1007/s11432-017-9259-0

1 Introduction

A coexistent structure of single carrier with frequency domain equalization (SC-FDE) and orthogonal frequency division multiplexing (OFDM) has been standardized in long-term evolution (LTE). However, to meet heterogeneous service requirements for the green 5G [1–3], the convergence of single carrier (SC) and multi-carrier (MC) such as vector-OFDM [4], generalized frequency division multiplexing [5, 6] and universal filtered multi-carrier [7], seems to be an alternative to traditional monotonous air interfaces. Therefore, a flexible waveform design with adjustable parameters, such as the fractional Fourier transform proposed in [8, 9] is needed to achieve the combined multi-object and multi-service. In addition, the possible SC/MC waveforms for 5G millimeter wave (mmWave) systems have been compared in [10] and the tradeoff view of a balanced solution has been put forward. In [11], diverse performances of OFDM/SC-FDE are compared under RF distortions in mmWave system. Considering the respective performance advantages of OFDM/SC-FDE schemes and the opposite characters between them, we could not easily obtain their performance merits simultaneously. Therefore, a unified waveform framework should be employed to achieve the smooth transition from OFDM to SC-FDE and vice versa.

As a fusion and also a bridge of SC and MC, hybrid carrier (HC) scheme based on weighted-type fractional Fourier transform (WFRFT) [12], not only has a compromising performance in many aspects,

* Corresponding author (email: meilin@hit.edu.cn)

such as spectrum efficiency (SE), peak to average power ratio (PAPR), energy efficiency (EE), and bit error rate (BER), but also outperforms SC/MC with narrow band interference [13] or over doubly selective fading channels [14]. Strong applicability is another superiority of WFRFT and HC scheme. The Fourier transform module in 5G candidate waveform can be substituted by WFRFT for performance improvement given in [15].

The minimum BERs of OFDM system with zero forcing (ZF) and minimum mean square error (MMSE) equalization are given in [16], where a class of channel independent optimal precoders are picked. In [17], the BER results are analytically given and a tradeoff appears between BER and bandwidth efficiency. BER analysis for SC-FDMA over Rayleigh fading channels with ideal linear FDE is achieved in [18] from the aspect of channel probability distribution. The performance of SC-FDE over underwater acoustic channels is analysed in [19] with one or more Doppler scaling factors. In addition, the equalization technique is also investigated in space time block code (STBC) based multiple-input multiple-output (MIMO) systems [20–22]. Specifically, STBC is exploited and integrated in SC and MC schemes with well compatibility as a performance improvement means. STBC-SC scheme with ZF/MMSE equalization is proposed in [23], which reveals code structure of two transmission moments. In [24], channel independent optimal precoder for STBC-OFDM is revealed.

Commendably, ZF and MMSE as the foremost linear block equalization methods also apply to hybrid carrier scheme. However, in most of the literatures about BER performance of HC scheme, simulations shoulder the main responsibility of demonstrating the advantage of HC and thus theoretical derivation is lacked to further explain this issue. Moreover, there is not any research on the combination of WFRFT and STBC with frequency domain equalization, nor any theoretical BER derivation in this respect. The main contribution of this paper illustrates the fusion property of HC scheme, which is a linear combination of SC and MC's features. Exact BER expressions of HC-FDE are firstly derived and considered as an example to display the linear fusion feature of WFRFT. Furthermore, a novel WFRFT precoded STBC structure is put forward to upgrade the performance over the fading channels, which is a generalized form of STBC-OFDM and STBC-SC systems.

2 Preliminary

2.1 WFRFT

α-th order WFRFT is defined as a linear summation of discrete time signal $x(n)$ and its discrete Fourier transform $X(n)$. Particularly, 4-WFRFT is expressed as

$$\mathscr{F}_{4W}^{\alpha}[x(n)] = w_0(\alpha)x(n) + w_1(\alpha)X(n) + w_2(\alpha)x(-n) + w_3(\alpha)X(-n), \tag{1}$$

where $x(-n)$ and $X(-n)$ are the reversed form of $x(n)$ and $X(n)$. The weighted parameters are denoted by

$$w_l(\alpha) = \cos\left[\frac{(\alpha-l)\pi}{4}\right]\cos\left[\frac{2(\alpha-l)\pi}{4}\right]\exp\left[\pm\mathrm{i}\frac{3(\alpha-l)\pi}{4}\right]. \tag{2}$$

For a vector $\boldsymbol{z}$, there is $\boldsymbol{z}_\alpha = \boldsymbol{W}(\alpha)\boldsymbol{z}$ after WFRFT, and the WFRFT matrix is shown as

$$\boldsymbol{W}(\alpha) = w_0(\alpha)\boldsymbol{I} + w_1(\alpha)\boldsymbol{F} + w_2(\alpha)\boldsymbol{\Gamma} + w_3(\alpha)\boldsymbol{\Gamma}\boldsymbol{F}, \tag{3}$$

where $\boldsymbol{I}$ denotes the $N\times N$ identity matrix. $\boldsymbol{F}$ denotes the $N\times N$ normalized Fourier matrix with $[\boldsymbol{F}]_{m,n} = 1/\sqrt{N}\cdot\exp[-\mathrm{j}2\pi mn/N]$ and $m,n = 0,\ldots,N-1$. $[\cdot]_{m,n}$ extracts the m-th row and n-th column entry from a matrix. $\langle\cdot\rangle_M$ denotes modulo-M calculation. The shift matrix $\boldsymbol{\Gamma}$ is defined by

$$\boldsymbol{\Gamma} = \begin{pmatrix} 1 & 0 & 0 & 0 & 0 \\ 0 & 0 & 0 & 0 & 1 \\ \vdots & \vdots & \vdots & \ddots & \vdots \\ 0 & 0 & 1 & 0 & 0 \\ 0 & 1 & 0 & 0 & 0 \end{pmatrix}. \tag{4}$$

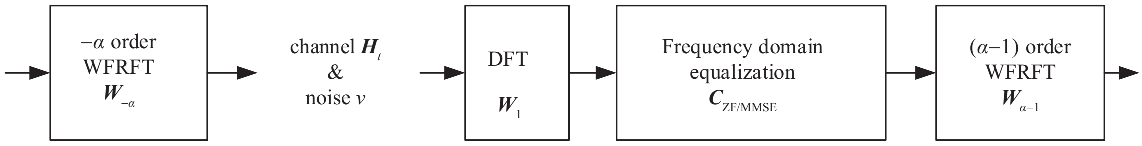

Figure 1 Framework of HC with FDE.

Moreover, $\boldsymbol{W}_\alpha$ obeys the following rules:

$$\boldsymbol{W}_{-\alpha} = \boldsymbol{W}_\alpha^{-1} = \boldsymbol{W}_\alpha^{\mathrm{H}}, \tag{5}$$

$$\boldsymbol{W}_{\alpha+\beta} = \boldsymbol{W}_\alpha \boldsymbol{W}_\beta = \boldsymbol{W}_\beta \boldsymbol{W}_\alpha, \tag{6}$$

which may contribute to the preferable understanding of WFRFT's concept.

2.2 HC system with FDE

The WFRFT-based communication system is depicted in Figure 1 with one $-\alpha$ order WFRFT module at the transmitter end. The WFRFT based HC system has a fusion structure of SC/OFDM due to the identity matrix (and also shift matrix) and Fourier matrix (and also inverse Fourier matrix) in the WFRFT's definition. At the receiver end, after the discrete Fourier transform (DFT), i.e., WFRFT with $\alpha = 1$, the signal is first transformed to the frequency domain for the FDE. According to (6), there is

$$\boldsymbol{W}_{-\alpha} = \boldsymbol{W}_{1-\alpha} \boldsymbol{W}_{-1} = \boldsymbol{W}_{1-\alpha} \boldsymbol{F}^{-1}. \tag{7}$$

Thus an $(\alpha - 1)$ order WFRFT is executed before decision. And it could be indicated that the HC system is also a WFRFT precoded OFDM system with precoding matrix $\boldsymbol{W}_{1-\alpha}$.

In the HC system, cyclic prefix is also employed to eliminate the inter block interference and make the channel matrix $\boldsymbol{H}_t$ be a circulant one. Thereby, the channel matrix $\boldsymbol{H}_t$ could be diagonalized by Fourier matrix, i.e.,

$$\boldsymbol{H}_t = \boldsymbol{F}^{-1} \boldsymbol{\Lambda}_f \boldsymbol{F}, \tag{8}$$

where $[\boldsymbol{\Lambda}_f]_{i,i} = \lambda_i$ $(i = 0, 1, \ldots, N-1)$ are the eigenvalues of $\boldsymbol{H}_t$, and the other entries of $\boldsymbol{\Lambda}_f$ equal 0. As a result, the simple frequency domain linear equalization could be implemented, no matter it is SC, MC or HC. Let $\boldsymbol{s}$ and $\boldsymbol{x}$ be the transmitted and received vector, respectively. There is

$$\boldsymbol{x} = \boldsymbol{W}_{\alpha-1} \boldsymbol{C}_{\mathrm{ZF/MMSE}} \boldsymbol{\Lambda}_f \boldsymbol{F} \boldsymbol{W}_{-\alpha} \boldsymbol{s} + \boldsymbol{W}_{\alpha-1} \boldsymbol{C}_{\mathrm{ZF/MMSE}} \boldsymbol{F} \boldsymbol{v}, \tag{9}$$

where $\boldsymbol{v}$ denotes additive white Gaussian noise (AWGN) with variance σ_v^2.

Let E_{savg} denote the average signal power of each modulated symbol, then the signal-to-noise ratio (SNR) is $\gamma = E_{\mathrm{savg}}/\sigma_v^2$. If squared M-quadrature amplitude modulation (QAM) is taken into consideration, there is $E_{\mathrm{savg}} = E_{\mathrm{bavg}} \cdot \log_2 M$ where E_{bavg} denotes the average energy per bit. The relationship between E_{savg} and $d_{\min}$ is shown as

$$E_{\mathrm{savg}} = d_{\min}^2 \cdot (M-1)/6. \tag{10}$$

Since the minimum distance $d_{\min}$ of the rectangular M-QAM modulation is 2, there is $E_{\mathrm{bavg}} = 1$ when $M = 4$ and $E_{\mathrm{bavg}} = 2.5$ when $M = 16$. Assuming perfect channel state information is available at the receiver, the equalization matrix is shown as $\boldsymbol{C}_{\mathrm{ZF}} = \boldsymbol{\Lambda}_f^{-1}$ and $\boldsymbol{C}_{\mathrm{MMSE}} = \boldsymbol{\Lambda}_f^*/(|\boldsymbol{\Lambda}_f|^2 + 1/\gamma)$.

2.3 Linear combination of SC and MC

Obviously, the HC-FDE system will degenerate to OFDM at α=1 and SC-FDE at α=0. Following the notion of HC, the relationship between SC and MC in the WFRFT's concept could be revealed by

$$W_{\mathrm{sc}}(\alpha) = |w_0(\alpha)|^2 + |w_2(\alpha)|^2 = |w_1(1-\alpha)|^2 + |w_3(1-\alpha)|^2, \tag{11a}$$

$$W_{\rm mc}(\alpha) = |w_1(\alpha)|^2 + |w_3(\alpha)|^2 = |w_0(1-\alpha)|^2 + |w_2(1-\alpha)|^2, \tag{11b}$$

where $W_{\rm mc}(\alpha)$ and $W_{\rm sc}(\alpha)$ denote the MC and SC components of HC system. Due to the unitary property of WFRFT, for arbitrary WFRFT order there is

$$W_{\rm sc}(\cdot) + W_{\rm mc}(\cdot) = 1. \tag{12}$$

With this combination, some convex optimization problems might be formalized. It could be an approach of optimum parameter selection for WFRFT, and moreover, degenerate to be an methodology for the comparisons between SC and MC. In Section 3, the SER/BER analysis of HC is presented as an example to reveal its hybrid form of SC and MC.

2.4 EE and SE of HC

Energy efficiency and spectrum efficiency are two critical indicators of communication systems. On one hand, compared to the poor power amplifier efficiency in MC system, the consumption of power amplifier in SC scheme is least due to its lowest PAPR, which is related with the energy efficiency [25]. The HC scheme has a compromised and variable PAPR, and thus it has a moderate energy efficiency between MC and SC schemes. On the other hand, compared to SC scheme, the HC system owns higher spectrum efficiency due to the MC component in it. Therefore, as a convergence of OFDM and SC schemes, the HC scheme has a tradeoff performance of energy efficiency and spectrum efficiency. Moreover, as a result of the adjustable order of WFRFT, the HC system could regulate its order to meet the diverse service requirements of green 5G.

Furthermore, due to the strong compatibility of HC scheme, EE and SE performance improvement methods, such as MIMO, are also applicable to HC system. For HC scheme itself with a stationary WFRFT order, there is also a tradeoff between EE and SE, which follows the analysis methods and performance rules of OFDM system. Therefore, some techniques about EE and SE in OFDM system given in [26–29], could also be considered and employed in HC system.

3 SER/BER analysis of HC with FDE

3.1 SER/BER over AWGN channel

Firstly, the SER of M-QAM modulation over an AWGN channel could be calculated by

$$\mathcal{P}_s = 4c_1 \cdot Q(\sqrt{c_2\gamma}) \times [1 - c_1 \cdot Q(\sqrt{c_2\gamma})], \tag{13}$$

where $c_1 = 1 - 1/\sqrt{M}$ and $c_2 = 3/(M-1)$. The Q function is defined as $Q(x) = 1/\sqrt{2\pi}\int_x^{\infty}\exp(-t^2/2){\rm d}t$ and $x \geqslant 0$. If Gray code is adopted, the BER $\mathcal{P}_b$ could be approximated to $\mathcal{P}_s/\log_2 M$ when γ is large enough. Therefore, the BER expression can be obtained after omiting the square of Q function, shown as

$$\mathcal{P}_b = 4c_1/\log_2 M \cdot Q(\sqrt{c_2\gamma}), \tag{14}$$

where the well-known analytical BER expression for quadrature phase shift keying (QPSK) could be gained at $M = 4$, i.e., $Q(\sqrt{\gamma})$.

3.2 ZF equalization

When ZF method is considered, no residual interference is left after equalization. As signals are energy invariant before and after equalization, the noise variance on each decision position becomes the determining factor.

To OFDM system, the noise variance on each subcarrier is independent to the others, which can be calculated as

$$\sigma^2_{v,\text{MC-ZF}}(i) = \sigma^2_v/|\lambda_i|^2. \tag{15}$$

It is proven in [16] that for any unitary precoder $\boldsymbol{T}$ of precoded OFDM system, the noise variance of the i-subchannel is given as

$$\sigma_{\boldsymbol{T}}^2(i) = \sigma_v^2 \sum_{n=0}^{N-1} \frac{|t_{n,i}|^2}{|\lambda_n|^2} = \sum_{n=0}^{N-1} |t_{n,i}|^2 \sigma_{v,\text{MC-ZF}}^2(n), \tag{16}$$

where $t_{n,i}$ denotes the (n,i) element of the precoder $\boldsymbol{T}$. The proposed HC system in Figure 1 could be regarded as a precoded OFDM system, and the precoder is $\boldsymbol{T} = \boldsymbol{W}_{1-\alpha}$ given in (7). Thus the noise variance of HC system is revealed as

$$\sigma_{\text{HC-ZF}}^2(i) = \sigma_v^2 \sum_{n=0}^{N-1} \frac{|W_{n,i}|^2}{|\lambda_n|^2} = \sum_{n=0}^{N-1} |W_{n,i}|^2 \sigma_{v,\text{MC-ZF}}^2(n), \tag{17}$$

where $W_{n,i}$ denotes the (n,i) element of precoder $\boldsymbol{W}_{1-\alpha}$.

In stark contrast to OFDM, the precoder of SC system is $\boldsymbol{T} = \boldsymbol{W}_1 = \boldsymbol{F}$ at α=0 and the elements of the precoder is calculated as

$$W_{n,i}^{\text{SC}} = 1/\sqrt{N} \cdot \exp[-\text{j}2\pi ni/N]. \tag{18}$$

Combining (17) and (18), we can derive that

$$\sigma_{v,\text{SC-ZF}}^2 = \frac{\sigma_v^2}{N} \cdot \sum_{n=0}^{N-1} |\lambda_n|^{-2} = \sigma_v^2 \cdot \text{E}[|\lambda_n|^{-2}]. \tag{19}$$

In SC system, the noise is evenly distributed to every symbol as a result of DFT operation, and thus the noise variances on each decision position are same.

As to the HC system, the α in precoder $\boldsymbol{W}_{1-\alpha}$ is a fraction. Combining (2) and (3), we can obtain that

$$\boldsymbol{W}_{1-\alpha}^{\text{HC}} = w_0(1-\alpha)\boldsymbol{I} + w_1(1-\alpha)\boldsymbol{F} + w_2(1-\alpha)\boldsymbol{\Gamma} + w_3(1-\alpha)\boldsymbol{\Gamma}\boldsymbol{F}. \tag{20}$$

It could be seen that $\boldsymbol{W}_{1-\alpha}^{\text{HC}}$ is composed of four parts: two for akin identity matrix and the other two for akin Fourier matrix. Therefore, the weighted noise of HC scheme also comes from four parts: two for SC scheme and the other two for MC scheme. According to the characteristic of the Gaussian random variable, the linear superposition of independent Gaussian random variables is still a Gaussian random variable and its variance is the sum of each part. Hence, the weighted noise variance on the decision position i of HC scheme is

$$\begin{aligned}\sigma_{v,\text{HC-ZF}}^2(i) &= W_{\text{mc}}(\alpha) \cdot \sigma_{v,\text{MC-ZF}}^2(i) + W_{\text{sc}}(\alpha) \cdot \sigma_{v,\text{SC-ZF}}^2 \\ &= \sigma_v^2 \cdot \left(W_{\text{mc}}(\alpha) \cdot |\lambda_i|^{-2} + W_{\text{sc}}(\alpha) \cdot \text{E}\left[|\lambda_n|^{-2}\right]\right),\end{aligned} \tag{21}$$

where $W_{\text{mc}}(\alpha)$ and $W_{\text{sc}}(\alpha)$ are given in (11). Substituting $\sigma_{v,\text{HC-ZF}}^2$ and γ into (13), the SER of M-QAM modulation with ZF equalization can be obtained by

$$\mathcal{P}_{s,\text{HC-ZF}} = \frac{4c_1}{N} \sum_{i=0}^{N-1} Q\left(\sqrt{\frac{c_2 E_{\text{savg}}}{\sigma_{v,\text{HC-ZF}}^2(i)}}\right) \times \left[1 - c_1 Q\left(\sqrt{\frac{c_2 E_{\text{savg}}}{\sigma_{v,\text{HC-ZF}}^2(i)}}\right)\right]. \tag{22}$$

The BER of M-QAM modulation with ZF equalization could be roughly estimated by $\mathcal{P}_b = \mathcal{P}_s / \log_2 M$, after abandoning the second Q function term when it is small enough. Ultimately, BER of HC with M-QAM modulation is gained by

$$\mathcal{P}_{b,\text{HC-ZF}} = \frac{1}{N} \sum_{i=0}^{N-1} \frac{4c_1}{\log_2 M} Q\left(\sqrt{\frac{c_2 \gamma}{W_{\text{mc}}(\alpha) \cdot |\lambda_i|^{-2} + W_{\text{sc}}(\alpha) \cdot \text{E}[|\lambda_n|^{-2}]}}\right). \tag{23}$$

From another point of view, BER of HC with ZF equalization could also be obtained more directly. Taking QPSK/4QAM as an example, BER of OFDM is the average of each subcarrier, expressed as

$$\mathcal{P}_{b,4,\text{MC-ZF}} = \frac{1}{N} \sum_{i=0}^{N-1} Q\left(\sqrt{\frac{E_{\text{savg}}}{\sigma_{v,\text{MC-ZF}}^2(i)}}\right) = \text{E}\left[Q\left(\sqrt{\gamma |\lambda_i|^2}\right)\right]. \tag{24}$$

On the contrary, SC system has the same BER for each decision position, that is

$$\mathcal{P}_{b,4,\text{SC-ZF}} = Q\left(\sqrt{\frac{E_{\text{savg}}}{\sigma^2_{v,\text{SC-ZF}}}}\right) = Q\left(\sqrt{\frac{\gamma}{\mathrm{E}\left[|\lambda_n|^{-2}\right]}}\right). \tag{25}$$

Taking the place of $\sigma^2_{v,\text{MC-ZF}}$ by $\sigma^2_{v,\text{HC-ZF}}$ in (24), there is

$$\mathcal{P}_{b,4,\text{HC-ZF}} = \frac{1}{N}\sum_{i=0}^{N-1} Q\left(\sqrt{\frac{\gamma}{W_{\text{mc}}(\alpha)\cdot|\lambda_i|^{-2} + W_{\text{sc}}(\alpha)\cdot\mathrm{E}[|\lambda_n|^{-2}]}}\right). \tag{26}$$

It is easy to verify that (26) is consistent with (23) when $M = 4$.

3.3 MMSE equalization

Although the BER analysis of HC scheme with ZF equalization is very simple, it is extremely complicated to directly present a BER expression for HC scheme with MMSE equalization due to its mutative signal power, affected by the other transmitted symbols. Fortunately, Lin et al. gave a general analytical BER in [16] for any linear precoding OFDM system with MMSE equalization and a unitary precoding matrix $\boldsymbol{T}$. Also taking QPSK as an example, there is

$$\mathcal{P}_{b,4,\text{T-MMSE}} = \frac{1}{N}\sum_{i=0}^{N-1} h\left(\sum_{n=0}^{N-1}\frac{|t_{n,i}|^2}{1+\gamma|\lambda_n|^2}\right). \tag{27}$$

The function $h(y)$ is defined as

$$h(y) = Q\left(\sqrt{y^{-1}-1}\right). \tag{28}$$

$\boldsymbol{T} = \boldsymbol{I}$ and $\boldsymbol{T} = \boldsymbol{F}$ represent OFDM and SC-FDE scheme, respectively. As there is only one non-zero entry equaling 1 (at i=n) in any column of the identity matrix $\boldsymbol{I}$, the BER of OFDM system could be given by

$$\begin{aligned}\mathcal{P}_{b,4,\text{MC-MMSE}} &= \frac{1}{N}\sum_{i=0}^{N-1} h\left(y_{\text{mc}}(i)\right) = \frac{1}{N}\sum_{i=0}^{N-1} h\left(\frac{1}{1+\gamma|\lambda_i|^2}\right)\\ &= \frac{1}{N}\sum_{i=0}^{N-1} Q\left(\sqrt{\gamma|\lambda_i|^2}\right) = \mathcal{P}_{b,4,\text{MC-ZF}}.\end{aligned} \tag{29}$$

For the SC-FDE system, any entry $|t_{n,i}|$ in a Fourier matrix $\boldsymbol{F}$ equals $1/\sqrt{N}$. Hence, the BER of SC-FDE system is

$$\mathcal{P}_{b,4,\text{SC-MMSE}} = h(y_{\text{sc}}) = \frac{1}{N}\sum_{i=0}^{N-1} h\left(\frac{1}{N}\sum_{n=0}^{N-1}\frac{1}{1+\gamma|\lambda_n|^2}\right) = h\left(\mathrm{E}\left[\frac{1}{1+\gamma|\lambda_n|^2}\right]\right). \tag{30}$$

From above, the BER of QPSK modulated OFDM system with MMSE equalization is equal to that with ZF equalization owing to same SNR $\gamma|\lambda_i|^2$ at the receiver. But in SC system, different equalization ways result in disparate BER performance because of evenly distributed noise and residual interference power.

According to the unitary property described in (5), the WFRFT matrix $\boldsymbol{W}_\alpha$ could also be regarded as a channel independent precoding matrix with the nature of $\boldsymbol{W}_\alpha\boldsymbol{W}_\alpha^{\mathrm{H}}$=$\boldsymbol{I}$. Thus the analytical BER expression of HC system could be derived from (27), through employing the linear combination of OFDM and SC-FDE precoding matrices. From the WFRFT definition in (1), one entry in $\boldsymbol{W}_{1-\alpha}$ could be divided into four parts, where entries from $\boldsymbol{I}$ and $\boldsymbol{\Gamma}$ constitute the MC component and entries from $\boldsymbol{F}$ and $\boldsymbol{\Gamma F}$ constitute the SC component. For the MC component, there are only two non-zero entries in a column, from $\boldsymbol{I}$ and $\boldsymbol{\Gamma}$ respectively. As to the SC component, absolute values of all the entries equal $1/\sqrt{N}$, no matter from $\boldsymbol{F}$ or $\boldsymbol{\Gamma F}$. Therefore, taking the weighting coefficients w_l into consideration, there is

$$\sum_{n=0}^{N-1}|t_{n,i}|^2 = \left[|w_0(1-\alpha)|^2 + |w_2(1-\alpha)|^2\right] + \frac{|w_1(1-\alpha)|^2 + |w_3(1-\alpha)|^2}{N}, \tag{31}$$

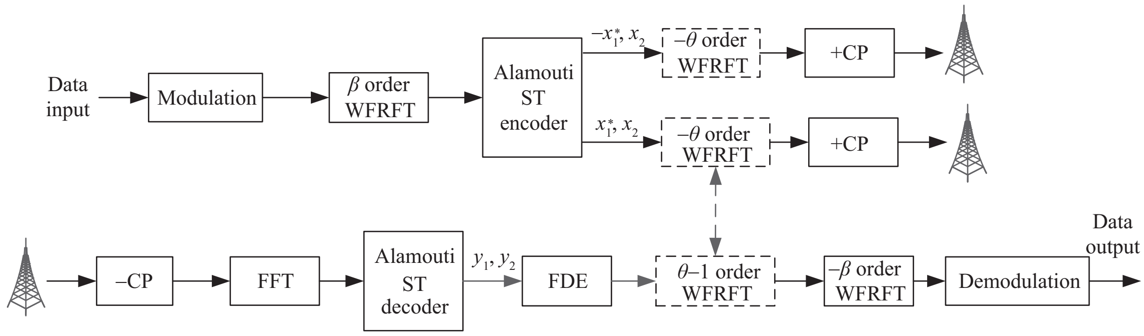

Figure 2 Framework of WFRFT precoded STBC-MC/SC-FDE system.

at $\boldsymbol{T} = \boldsymbol{W}_{1-\alpha}$. By substituting (31) into (27), we finally get the BER expression of HC system with MMSE equalization,

$$\begin{aligned}\mathcal{P}_{b,4,\text{HC-MMSE}} &= \frac{1}{N}\sum_{i=0}^{N-1} h\left(y_{\text{hc}}(i)\right) = \frac{1}{N}\sum_{i=0}^{N-1} h\left(W_{\text{mc}}(\alpha)\cdot y_{\text{mc}}(i) + W_{\text{sc}}(\alpha)\cdot y_{\text{sc}}\right)\\ &= \frac{1}{N}\sum_{i=0}^{N-1} h\left(\frac{W_{\text{mc}}(\alpha)}{1+\gamma|\lambda_i|^2} + \text{E}\left[\frac{W_{\text{sc}}(\alpha)}{1+\gamma|\lambda_n|^2}\right]\right)\\ &= \frac{1}{N}\sum_{i=0}^{N-1} Q\left(\sqrt{\left(\frac{W_{\text{mc}}(\alpha)}{1+\gamma|\lambda_i|^2} + \text{E}\left[\frac{W_{\text{sc}}(\alpha)}{1+\gamma|\lambda_n|^2}\right]\right)^{-1} - 1}\right).\end{aligned} \tag{32}$$

Combining (13) and (32), SER of M-QAM modulation with MMSE equalization is given by

$$\mathcal{P}_{s,\text{HC-MMSE}} = \frac{1}{N}\sum_{i=0}^{N-1} 4c_1 Q\left(\sqrt{c_2\left(y_{\text{hc}}^{-1}(i) - 1\right)}\right) \times \left[1 - c_1 Q\left(\sqrt{c_2\left(y_{\text{hc}}^{-1}(i) - 1\right)}\right)\right]. \tag{33}$$

After that, BER of M-QAM modulation is derived through giving up high order Q function term, which is expressed by

$$\mathcal{P}_{b,\text{HC-MMSE}} = \frac{1}{N}\sum_{i=0}^{N-1} \frac{4c_1}{\log_2 M} Q\left(\sqrt{c_2\left(y_{\text{hc}}^{-1}(i) - 1\right)}\right), \tag{34}$$

which matches with (32) at M=4.

4 BER analysis of WFRFT precoded STBC-MC/SC-FDE system

4.1 STBC-MC/SC-FDE system framework

The WFRFT-STBC-SC/MC-FDE system is proposed with two separately WFRFT modules at the transmitter and receiver. As shown in Figure 2, the STBC coding is operated in time domain or frequency domain, which is decided by the selection of θ, i.e., 0 or 1. Correspondingly, the STBC decoding is employed in frequency domain due to the FFT before it. According to properties of STBC, if the coding and decoding operations are carried out in different domains, the data should be reversed before transmitting owing to the duality of data reversion in time domain and data conjugation in frequency domain.

As a result of the adjustable WFRFT parameters, the STBC-OFDM-FDE system and STBC-SC-FDE system are two special cases of the proposed system. The β order WFRFT is a precoder with the general parameter selection in [0,1]. If there is no WFRFT precoder, i.e., β=0, the proposed system framework in Figure 2 is a STBC-OFDM system at θ=1 or a STBC-SC-FDE system at θ=0. Further, at β=1 i.e., $\boldsymbol{W}_\beta = \boldsymbol{F}$, it is a DFT precoded OFDM at θ=1 or a DFT precoded SC system at θ=0. Therefore, as given in Table 1, the proposed STBC based system appears a MC feature at β=0, θ=1, a SC feature at β=0,

Table 1 The relationship between parameters and carrier feature

WFRFT parameters	Carrier feature
β=0, θ=1	STBC-MC
$\beta \in (0,1)$, θ=1	WFRFT-STBC-MC (HC)
β=1, θ=1	DFT-STBC-MC (SC)
β=0, θ=0	STBC-SC
$\beta \in (0,1)$, θ=0	WFRFT-STBC-SC (HC)
β=1, θ=0	DFT-STBC-SC (MC)

θ=0, a DFT-s-OFDM feature (appear SC characteristic) at β=1, θ=1 and a DFT spread SC feature (appear MC characteristic) at β=1, θ=0. Moreover, at fractional order β, it is a WFRFT precoded OFDM or SC system. Although the performances of WFRFT-STBC-OFDM and WFRFT-STBC-SC systems are different, they both appear a HC feature at fractional β. Actually, their BER performances are complementary illustrated by following proof.

4.2 STBC system model

In Alamouti STBC system, two successive symbols $\boldsymbol{x}_1$ and $\boldsymbol{x}_2$ are coded according to the space-time codeword matrix. In the first time duration, $\boldsymbol{x}_1$ and $\boldsymbol{x}_2$ are transmitted from the two antennas. The conjugation symbols $-\boldsymbol{x}_2^*$ and $\boldsymbol{x}_1^*$ are conveyed in the second duration. Note that, data need to be reversed in STBC-SC-FDE scheme. Meanwhile, channel state information (CSI) is presumed same in two time durations. The transmitted signal can be expressed as

$$\begin{cases} \boldsymbol{y}_1 = \boldsymbol{\Lambda}_1\boldsymbol{x}_1 + \boldsymbol{\Lambda}_2\boldsymbol{x}_2 + \boldsymbol{v}_1, \\ \boldsymbol{y}_2 = \boldsymbol{\Lambda}_2\boldsymbol{x}_1^* - \boldsymbol{\Lambda}_1\boldsymbol{x}_2^* + \boldsymbol{v}_2, \end{cases} \tag{35}$$

where $\boldsymbol{v}_1$ and $\boldsymbol{v}_2$ are uncorrelated zero-mean complex Gaussian random vectors with the variance $\sigma_{v_1}^2$ and $\sigma_{v_2}^2$, respectively. As given in (8), channel transmit matrix $\boldsymbol{H}_1$ and $\boldsymbol{H}_2$ can be transformed into a cyclic matrix through the CP and then diagonalized by Fourier matrix. $\boldsymbol{\Lambda}_1$ and $\boldsymbol{\Lambda}_2$ are diagonal matrix constructed by the eigenvalues of $\boldsymbol{H}_1$ and $\boldsymbol{H}_2$, denoted as $\boldsymbol{H}_1 = \boldsymbol{F}^{-1}\boldsymbol{\Lambda}_1\boldsymbol{F}$ and $\boldsymbol{H}_2 = \boldsymbol{F}^{-1}\boldsymbol{\Lambda}_2\boldsymbol{F}$.

After the conjugation of signal in the second moment, matrix form of the two formulas is obtained as

$$\begin{bmatrix} \boldsymbol{y}_1 \\ \boldsymbol{y}_2^* \end{bmatrix} = \begin{bmatrix} \boldsymbol{\Lambda}_1 & \boldsymbol{\Lambda}_2 \\ \boldsymbol{\Lambda}_2^* & -\boldsymbol{\Lambda}_1^* \end{bmatrix} \cdot \begin{bmatrix} \boldsymbol{x}_1 \\ \boldsymbol{x}_2 \end{bmatrix} + \begin{bmatrix} \boldsymbol{v}_1 \\ \boldsymbol{v}_2^* \end{bmatrix}. \tag{36}$$

When STBC decoding at the receiver is considered, channel transmit matrix is multiplied by its conjugate transpose form, shown as

$$\begin{bmatrix} \boldsymbol{\Lambda}_1^* & \boldsymbol{\Lambda}_2 \\ \boldsymbol{\Lambda}_2^* & -\boldsymbol{\Lambda}_1 \end{bmatrix}. \tag{37}$$

Here we assume that the CSI is known at the receiver. Therefore, the relationship between input and output ends is shown as

$$\begin{bmatrix} \tilde{\boldsymbol{y}}_1 \\ \tilde{\boldsymbol{y}}_2 \end{bmatrix} = (|\boldsymbol{\Lambda}_1|^2 + |\boldsymbol{\Lambda}_2|^2) \cdot \begin{bmatrix} \boldsymbol{x}_1 \\ \boldsymbol{x}_2 \end{bmatrix} + \begin{bmatrix} \tilde{\boldsymbol{v}}_1 \\ \tilde{\boldsymbol{v}}_2^* \end{bmatrix}. \tag{38}$$

Further, $\boldsymbol{\Phi}$ is defined as

$$\boldsymbol{\Phi} = |\boldsymbol{\Lambda}_1|^2 + |\boldsymbol{\Lambda}_2|^2, \tag{39}$$

where $[\boldsymbol{\Phi}]_{k,k} = |\phi_k|^2$ $(k = 0, 1, \ldots, N-1)$.

4.3 ZF receiver

4.3.1 $\theta = 1$

At θ=1, the proposed system is simplified to a WFRFT precoded STBC-OFDM system. According to (38), the received signal could be expressed as

$$\tilde{\boldsymbol{y}}_q = \boldsymbol{W}_{-\beta}\boldsymbol{C}_{\mathrm{ZF}}\boldsymbol{\Phi}\boldsymbol{W}_{\beta}\boldsymbol{x}_q + \boldsymbol{W}_{-\beta}\boldsymbol{C}_{\mathrm{ZF}}\boldsymbol{F}\boldsymbol{v}_q = \boldsymbol{x}_q + \hat{\boldsymbol{v}}_q, \tag{40}$$

where $q = 1, 2$ and $\hat{\boldsymbol{v}}_q = \boldsymbol{W}_{-\beta}\boldsymbol{C}_{\mathrm{ZF}}\boldsymbol{F}\boldsymbol{v}_q$. The ZF receiver is denoted as

$$\boldsymbol{C}_{\mathrm{ZF}} = \frac{1}{\boldsymbol{\Phi}}. \tag{41}$$

At β=0, from (24), the BER of STBC-OFDM system is derived as

$$\mathcal{P}_{b,4,\text{STBC-MC-ZF}} = \frac{1}{N}\sum_{k=0}^{N-1} Q\left(\sqrt{\frac{E_{\mathrm{savg}}}{\sigma^2_{v,\text{STBC-MC-ZF}}(k)}}\right) = \mathrm{E}\left[Q\left(\sqrt{\gamma|\phi_k|^2}\right)\right]. \tag{42}$$

Furthermore, the BER of WFRFT precoded STBC-MC system could be obtained as

$$\mathcal{P}_{b,\text{WFRFT-STBC-MC-ZF},\beta} = \frac{1}{N}\sum_{k=0}^{N-1}\frac{4c_1}{\log_2 M}Q\left(\sqrt{\frac{c_2\gamma}{W_{\mathrm{mc}}(1-\beta)\cdot|\phi_k|^{-2} + W_{\mathrm{sc}}(1-\beta)\cdot\mathrm{E}[|\phi_m|^{-2}]}}\right), \tag{43}$$

where index m follows the way in (23). For Figures 1 and 2, the WFRFT precoder is $\boldsymbol{W}_{1-\alpha}$ and $\boldsymbol{W}_{\beta}$, respectively. Thus we obtain $W_{\mathrm{mc}}(1-\beta) = |w_0(\beta)|^2 + |w_2(\beta)|^2$ and $W_{\mathrm{sc}}(1-\beta) = |w_1(\beta)|^2 + |w_3(\beta)|^2$ after substituting $(1-\beta)$ into (11).

At β=1 of (43), the BER of DFT spread STBC-OFDM system is calculated as

$$\mathcal{P}_{b,\text{DFT-STBC-MC-ZF}} = \frac{1}{N}\sum_{k=0}^{N-1}\frac{4c_1}{\log_2 M}Q\left(\sqrt{\frac{c_2\gamma}{\mathrm{E}[|\phi_m|^{-2}]}}\right) = \frac{4c_1}{\log_2 M}Q\left(\sqrt{\frac{c_2\gamma}{\mathrm{E}[|\phi_m|^{-2}]}}\right). \tag{44}$$

4.3.2 $\theta = 0$

At θ=0, the proposed system is simplified to a WFRFT precoded STBC-SC-FDE system. If we assume that the transmitted signals on two antennas at time p are $\boldsymbol{x}_{p,q}(u), u = 0, 1, \ldots, N-1$. Thus, at the next time $p+1$, the transmitted signals are given as

$$\begin{aligned} \boldsymbol{x}_{p+1,1}(u) &= -\boldsymbol{x}_{p,2}((-u)_N)^*, \\ \boldsymbol{x}_{p+1,2}(u) &= \boldsymbol{x}_{p,1}((-u)_N)^*, \end{aligned} \tag{45}$$

where $(\cdot)_N$ denotes the modulo N operation. In this way, the performance of Alamouti coding in time domain equals to that in frequency domain. The receiver signal can be expressed as

$$\tilde{\boldsymbol{y}}_q = \boldsymbol{x}_q + \boldsymbol{W}_{-\beta}\boldsymbol{F}_{-1}\boldsymbol{C}_{\mathrm{ZF}}\boldsymbol{F}\boldsymbol{v}_q. \tag{46}$$

At β=0, the noise power could be obtained from (19),

$$\sigma^2_{v,\text{STBC-SC-ZF}} = \frac{\sigma_v^2}{N}\cdot\sum_{m=0}^{N-1}|\phi_m|^{-2} = \sigma_v^2\cdot\mathrm{E}\left[|\phi_m|^{-2}\right]. \tag{47}$$

Therefore, the BER of STBC-SC-ZF system is derived as

$$\mathcal{P}_{b,4,\text{STBC-SC-ZF}} = Q\left(\sqrt{\frac{E_{\mathrm{savg}}}{\sigma^2_{v,\text{STBC-SC-ZF}}}}\right) = Q\left(\sqrt{\frac{\gamma}{\mathrm{E}\left[|\phi_m|^{-2}\right]}}\right) = \mathcal{P}_{b,4,\text{DFT-STBC-MC-ZF}}. \tag{48}$$

At β=1, the equivalent noise of DFT-STBC-SC-ZF system equals to the uncoded OFDM system. Thus the noise power could be obtained from (15), shown as

$$\sigma^2_{v,\text{DFT-STBC-SC-ZF}}(k) = \sigma^2_v/|\phi_k|^2. \tag{49}$$

According to the linear combination feature of WFRFT, the noise power of WFRFT-STBC-SC-ZF system is

$$\sigma^2_{v,\text{WFRFT-STBC-SC-ZF}}(k) = \sigma^2_v \cdot \left(W_{\text{mc}}(\beta) \cdot |\phi_k|^{-2} + W_{\text{sc}}(\beta) \cdot \text{E}\left[|\phi_m|^{-2}\right]\right). \tag{50}$$

Therefore, the BER of WFRFT-STBC-SC-ZF system is derived as

$$\begin{aligned} &\mathcal{P}_{b,\text{WFRFT-STBC-SC-ZF},\beta} \\ &= \frac{1}{N}\sum_{k=0}^{N-1}\frac{4c_1}{\log_2 M}Q\left(\sqrt{\frac{c_2\gamma}{W_{\text{mc}}(\beta)\cdot|\phi_k|^{-2} + W_{\text{sc}}(\beta)\cdot\text{E}[|\phi_m|^{-2}]}}\right). \end{aligned} \tag{51}$$

Combining (43) with (51), there is

$$\mathcal{P}_{b,\text{WFRFT-STBC-SC-ZF},\beta} = \mathcal{P}_{b,\text{WFRFT-STBC-MC-ZF},1-\beta}. \tag{52}$$

For the WFRFT precoded STBC-SC system (θ=0), the carrier scheme transforms from SC to MC with the change of β from 0 to 1. On the contrary, for the WFRFT precoded STBC-MC system (θ=1), the carrier scheme alters from SC to MC with the change of β from 1 to 0. Therefore, there is a complementary relationship between two WFRFT precoded systems. Since HC is constituted by the corresponding carrier components of SC and MC, a relationship of WFRFT precoding order between two systems could be obtained in (52). At β=1, there is

$$\begin{aligned} &\mathcal{P}_{b,\text{DFT-STBC-SC-ZF}} \\ &= \mathcal{P}_{b,\text{STBC-MC-ZF}} = \frac{1}{N}\sum_{k=0}^{N-1}\frac{4c_1}{\log_2 M}Q\left(\sqrt{c_2\gamma|\phi_k|^2}\right). \end{aligned} \tag{53}$$

4.4 MMSE receiver

The BER performance of STBC-MMSE system can be derived through jointing the BER derivations of HC-MMSE system in (34) and WFRFT-STBC-SC/MC-ZF system in (51), (52). Note that, as a result of the STBC coding and decoding, the MMSE equalization matrix is rewritten as

$$\boldsymbol{C}_{\text{MMSE}} = \frac{1}{\boldsymbol{\Phi} + 1/\gamma}. \tag{54}$$

Comparing MMSE equalization with ZF equalization, from (52), we get

$$\mathcal{P}_{b,\text{WFRFT-STBC-SC-MMSE},\beta} = \mathcal{P}_{b,\text{WFRFT-STBC-MC-MMSE},1-\beta}. \tag{55}$$

Combined with (34), there is

$$\begin{aligned} &\mathcal{P}_{b,\text{WFRFT-STBC-SC-MMSE},\beta} \\ &= \mathcal{P}_{b,\text{WFRFT-STBC-MC-MMSE},1-\beta} \\ &= \frac{1}{N}\sum_{k=0}^{N-1}\frac{4c_1}{\log_2 M}Q\left(\sqrt{c_2\left(y^{-1}_{\text{WFRFT-STBC}}(k)-1\right)}\right) \\ &= \frac{1}{N}\sum_{k=0}^{N-1}\frac{4c_1}{\log_2 M}Q\left(\sqrt{c_2\cdot\left(\frac{W_{\text{mc}}(\beta)}{1+\gamma|\phi_k|^2} + \text{E}\left[\frac{W_{\text{sc}}(\beta)}{1+\gamma|\phi_m|^2}\right]\right)^{-1} - c_2}\right). \end{aligned} \tag{56}$$

According to the selected values of θ and β in (56), we can acquire the BER expressions of diverse WFRFT-STBC-SC/MC-MMSE systems.

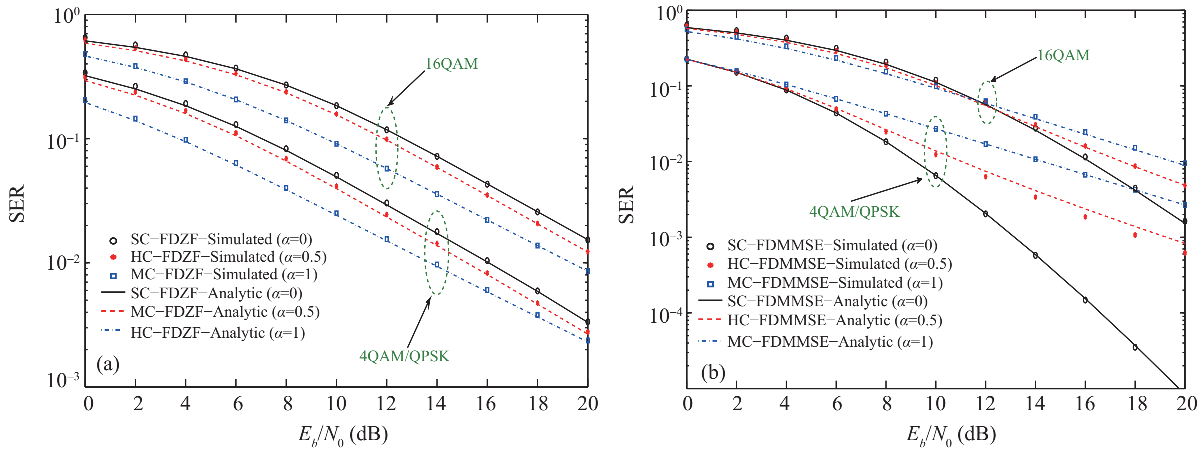

Figure 3 (Color online) SER of HC system with frequency domain ZF/MMSE equalization over ITU Ped-B channel: markers denote the simulation results and lines denote the analytic results. (a) ZF; (b) MMSE.

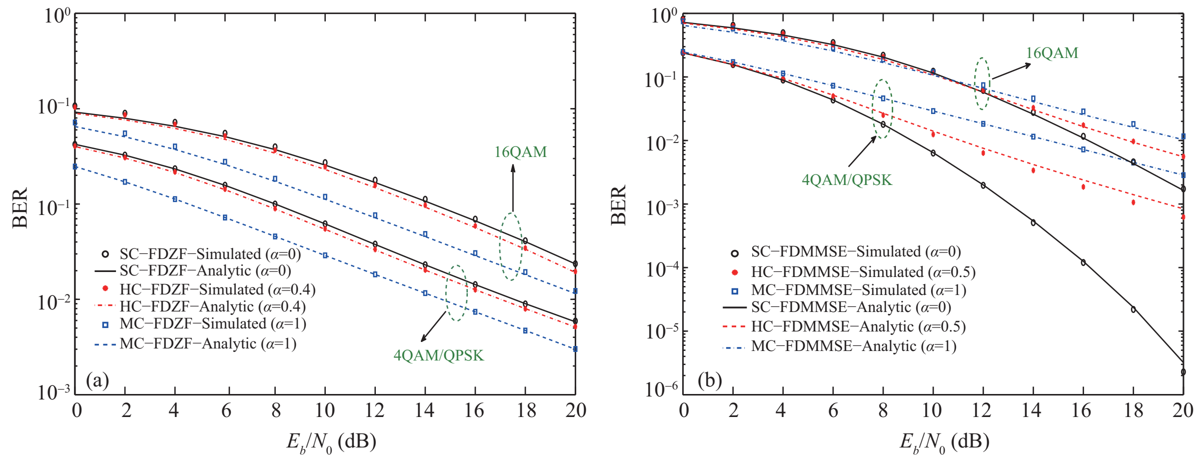

Figure 4 (Color online) BER of HC system with frequency domain ZF/MMSE equalization over ITU Ped-B channel: markers denote the simulation results and lines denote the analytic results. (a) ZF; (b) MMSE.

5 Simulation results and discussion

In this section, we verify the SER expressions in (22), (33) and BER expressions in (23), (34) through Monte Carlo simulations over the ITU Ped-B channel. The relative delay of each path is [0, 100, 200, 300, 500, 700] ns, and average power of each path is [0, −3.6, −7.2, −10.8, −18, −25.2] dB. The chip rate is 10 Mcps and the number of subcarriers N in one block is 512. The SERs of HC with ZF and MMSE equalization are shown in Figure 3. In order to guarantee the randomness of fading channels, 2000 independent channels are generated for each situation, and hundreds of simulations have been done over each channel. The averages of calculation results of (22) and (33) for each independent channel yield the analytical results in the figures. Similarly, the simulated and derived BER results in (23) and (34) are revealed in Figure 4.

After the linear combination feature of hybrid carrier scheme is illustrated through the SER/BER performance of HC-FDE, this characteristic is also maintained in STBC hybrid carrier system. In Figure 5, the BER expressions in (51) and (56) are verified over the fixed fading channels. The two channel impulse response is [0.8639, −0.4319, 0.2592] and [0.7274 −0.5819 0.3637], respectively. The delays are with [0, 4, 9] and [0, 2, 7] chips. The WFRFT precoded STBC-MC and STBC-SC systems appear consistent performance at matched β and θ. Both figures show that the analytical BERs match well with the simulation ones.

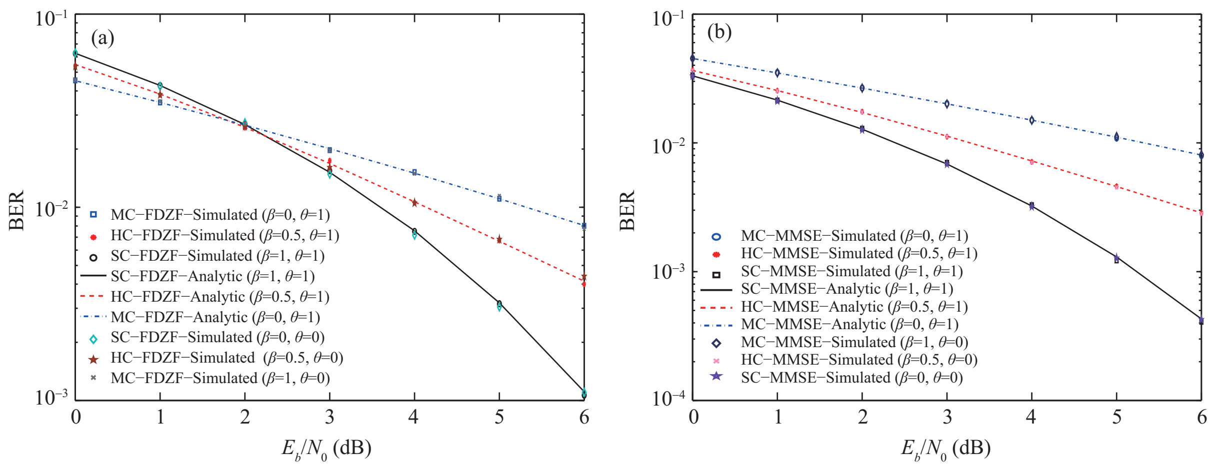

Figure 5 (Color online) BER of QPSK modulated WFRFT-STBC-MC/SC system with frequency domain ZF/MMSE equalization: markers denote the simulation results and lines denote the analytic results. (a) ZF; (b) MMSE.

6 Conclusion

In this paper, the linear combination of SC and MC schemes is illustrated through the BER analysis of hybrid carrier system based on WFRFT with frequency domain equalization, which contributes to the future waveform design and compatibility in 5G. Specifically, the analytical SER/BER expressions of HC-FDE system are derived and verified by simulation results. Moreover, the linear combination characteristics of WFRFT are also achieved in the STBC hybrid carrier system.

Acknowledgements This work was supported by National Natural Science Foundation of China (Grant No. 61671179), National Basic Research Program of China (Grant No. 2013CB329003), and Science and Technology on Information Transmission and Dissemination in Communication Networks Laboratory (Grant No. EX156410046).

References

1 Ge X H, Chen J Q, Wang C X, et al. 5G green cellular networks considering power allocation schemes. Sci China Inf Sci, 2016, 59: 022308
2 Ge X H, Yang J, Gharavi H, et al. Energy efficiency challenges of 5G small cell networks. IEEE Commun Maga, 2017, 55: 184–191
3 Zhou S, Zhao T, Niu Z S, et al. Software-defined hyper-cellular architecture for green and elastic wireless access. IEEE Commun Maga, 2016, 54: 12–19
4 Li Y, Ngebani I, Xia X G, et al. On performance of vector OFDM with linear receivers. IEEE Trans Signal Process, 2012, 60: 5268–5280
5 Michailow N, Matthe M, Gaspar I, et al. Generalized frequency division multiplexing for 5th generation cellular networks. IEEE Trans Commun, 2014, 62: 3045–3061
6 Han S, Sung Y, Lee Y H. Filter design for generalized frequency-division multiplexing. IEEE Trans Signal Process, 2017, 65: 1644–1659
7 Wild T, Schaich F, Chen Y. 5G air interface design based on universal filtered (UF-)OFDM. In: Proceedings of International Conference on Digital Signal Processing, Hong Kong, 2014. 699–704
8 Huan H, Shi P F, Yan X D, et al. Generalized spatial representation for digital modulation and its potential application. Sci China Inf Sci, 2016, 59: 122303
9 Kang X, Tao R, Zhang F. Multiple-parameter discrete fractional transform and its applications. IEEE Trans Signal Process, 2016, 64: 3402–3417
10 Ibars C, Kumar U, Niu H, et al. A comparison of waveform candidates for 5G millimeter wave systems. In: Proceedings of the 49th Asilomar Conference on Signals, Systems and Computers, Pacific Grove, 2015. 1747–1751
11 Khansefid A, Minn H, Zhan Q, et al. Waveform parameter design and comparisons for millimeter-wave massive MIMO systems with RF distortions. In: Proceedings of IEEE Globecom Workshops, Washington, 2016. 1–6
12 Mei L, Sha X J, Ran Q W, et al. Research on the application of 4-weighted fractional fourier transform in communication system. Sci China Inf Sci, 2010, 53: 1251–1260
13 Mei L, Zhang Q Y, Sha X J, et al. WFRFT precoding for narrowband interference suppression in DFT-based block transmission systems. IEEE Commun Lett, 2013, 17: 1916–1919

14 Hui Y, Li B, Tong Z. 4-weighted fractional Fourier transform over doubly selective channels and optimal order selecting algorithm. Electron Lett, 2015, 51: 177–179

15 Wang Z D, Mei L, Wang X L, et al. Bit error rate analysis of generalised frequency division multiplexing with weighted-type fractional Fourier transform precoding. IET Commun, 2017, 11: 916–924

16 Lin Y P, Phoong S M. BER minimized OFDM systems with channel independent precoders. IEEE Trans Signal Process, 2003, 51: 2369–2380

17 Ohno S. Performance of single-carrier block transmissions over multipath fading channels with linear equalization. IEEE Trans Signal Process, 2006, 54: 3678–3687

18 Sanchez-sanchez J J, Fernandez-plazaola U, Aguayo-torres M C. BER analysis for SC-FDMA over rayleigh fading channels. In: Proceedings of International Conference on Broadband and Biomedical Communication, Melbourne, 2011. 43–47

19 Daoud S, Ghrayeb A. Using resampling to combat doppler scaling in UWA channels with single-carrier modulation and frequency-domain equalization. IEEE Trans Veh Tech, 2016, 65: 1261–1270

20 Kong D J, Xiang X G, Jiang T. An Alamouti coded CP-FBMC-MIMO system with two transmit antennas. Sci China Inf Sci, 2015, 58: 102306

21 Feng W, Wang Y, Ge N, et al. Virtual MIMO in multi-cell distributed antenna systems: coordinated transmissions with large-scale CSIT. IEEE J Sel Area Commun, 2013, 31: 2067–2081

22 Kan H B, Liu X D, Han G Y. On the criteria for designing complex orthogonal space-time block codes. Sci China Inf Sci, 2016, 59: 082303

23 Al-Dhahir N. Single-carrier frequency-domain equalization for space-time block-coded transmissions over frequency-selective fading channels. IEEE Commun Lett, 2001, 5: 304–306

24 Chung Y H, Phoong S M. Unitary precoders for ST-OFDM systems using Alamouti STBC. IEEE Trans Circ Syst I, 2008, 55: 2860–2869

25 Yoshizawa R, Ochiai H. Energy efficiency improvement of coded OFDM systems based on PAPR reduction. IEEE Syst J, 2017, 11: 717–728

26 Li C G, Li Y S, Song K, et al. Energy efficient design for multiuser downlink energy and uplink information transfer in 5G. Sci China Inf Sci, 2016, 59: 022305

27 Zhang Y H, Cui Q M, Wang N, et al. Energy-efficient resource allocation for hybrid bursty services in multi-relay OFDM networks. Sci China Inf Sci, 2017, 60: 102304

28 Hu H, Zhang H, Liang Y C. On the spectrum- and energy-efficiency tradeoff in cognitive radio networks. IEEE Trans Commun, 2016, 64: 490–501

29 Zhao L, Li K, Zheng K, et al. An analysis of the tradeoff between the energy and spectrum efficiencies in an uplink massive MIMO-OFDM system. IEEE Trans Circ Syst II, 2015, 62: 291–295